J. exp. Biol. 142, 87–95 (1989)
Printed in Great Britain © *The Company of Biologists Limited 1989*

INERTIAL AND AERODYNAMIC TORQUES ON THE WINGS OF DIPTERA IN FLIGHT

BY A. ROLAND ENNOS*

Department of Biological Sciences, Hatherly Laboratories, University of Exeter, Prince of Wales Road, Exeter EX4 4PS

Accepted 5 September 1988

Summary

1. The magnitude and distribution of the torques caused by inertial and aerodynamic forces on the wings of Diptera in flight are calculated.

2. The bending torque at stroke reversal due to the inertia of the virtual mass of air bound to the wing is only slightly less than the torque due to the inertia of the wing mass itself. The maximum inertial torque due to both wing mass and virtual mass is usually slightly greater than the maximum aerodynamic torque encountered by the wings.

3. Bending torques decrease rapidly away from the wing base.

4. Pitching torques are much smaller than bending torques at the wing base, but do not decrease much until near the tip.

5. The pattern of loading affects the wing design. Wings are thicker nearer the base to resist bending, but thin and light near the tip to minimize inertial energy expenditure. Their open, corrugated structure resists bending, while allowing them to be twisted as a result of the weak pitching moments.

Introduction

The torques generated by insects at the wing base to overcome aerodynamic and inertial forces have been quite widely studied in the context of flight energetics (Weis-Fogh, 1973; Ellington, 1984*d*). The torques that will be set up all the way along the wing as a consequence, however, have largely been ignored: only Pennycuick (1967) seems to have examined the bending and pitching torques set up in a wing during flight, and only at certain points of the wings of his pigeons.

The bending torques produced in flight will vary both temporally and spatially. Inertial forces will predominate at stroke reversal when acceleration is greatest. Aerodynamic forces, however, will predominate in the middle of each halfstroke during normal horizontal stroke plane hovering (Weis-Fogh, 1973), whether circulation is produced by quasi-steady or rotational mechanisms, when the wing

* Present address: Department of Biological Science, University of York, Heslington, York YO1 5DD

Key words: Diptera, wing, flight, bending, torsion.

velocity is greatest. Both forces vary along the wing. This paper seeks to investigate the relative magnitudes of the bending torques due to inertia, both of the wing itself and of the virtual mass of air bound to the wing (Vogel, 1962; Ellington, 1984*a*), and those due to aerodynamic forces, and to examine their distribution along the wing.

Since the centre of mass of insect wings is located behind the torsional axis (Norberg, 1972), acceleration of the wings should also tend to set up inertial pitching torques which would tend to twist the wing. At stroke reversal, however, when these torques would be set up, the inertia instead causes the wings to rotate by over 90° at the torsionally compliant wing base (Ennos, 1987) into the correct orientation for the coming halfstroke. Inertial pitching moments are therefore ignored in this paper. I have shown elsewhere (Ennos, 1988*b*) that these inertial effects are sufficient to cause the rotational velocities of the wing which are observed at stroke reversal.

The chordwise centre of pressure of insect wings is generally behind the torsional axis (Norberg, 1972), so aerodynamic forces will also produce pitching torques along the wings. During the middle of each halfstroke the wing pitch is more or less constant, showing that the pitching torques produced then are equal to the restoring torque produced by the compliant wing base (Ennos, 1987). The magnitude and distribution of the pitching torques set up by aerodynamic forces at this time were investigated.

The distribution of torques will be very important in determining the wing design: insect wings generally withstand the torques that are produced in flight without noticeable bending, but they are generally twisted nose-down along their length during the downstroke (Wootton, 1981; Ellington, 1984*b*). A wing of optimal design would be as light as possible, to increase the energetic efficiency of flight, while combining adequate bending and torsional stiffness.

Materials and methods

Five species of flies were investigated: the hoverfly *Eristalis tenax* (L.); the March fly *Bibio marci* (L.); the bluebottle, *Calliphora vicina* Robineau-Desvoidy; the conopid fly, *Conops strigata* Wied. in Meig.; and the crane fly *Tipula paludosa* Meig.

Information that I had obtained on the morphology and kinematics of free flight of these species (Ennos, 1989) was used to calculate the torque distribution along the wings in flight due to both inertial and aerodynamic forces.

To simplify the calculations, several assumptions were made. Measurements of wing acceleration and velocity from kinematic records would be subject to large errors, so it was assumed that the wings oscillated along the stroke plane with simple harmonic motion. The actual kinematics (Ennos, 1989) were very similar to simple harmonic motion, as were those observed in free flight by Ellington (1984*b*) and Dudley (1987). Acceleration at the ends of the beat was usually higher than in simple harmonic motion and peak velocity lower. This would mean that my

analysis would underestimate inertial torques and overestimate aerodynamic torques.

To calculate aerodynamic torques it was further assumed that the wings produced equal lift on each stroke and did so using the quasi-steady mechanism, in which the lift produced is proportional to the square of the local velocity. The quasi-steady account of insect flight is increasingly under attack (Ellington, 1984*b*; Dudley, 1987; Ennos, 1989), but remains the only mechanism yielding information about the spatial and temporal distribution of force on the wing. Furthermore, since the average force produced by the wings is known (lift must balance the weight of the insect in flight), the estimates of the peak force and torque that the quasi-steady assumption yields will be of the correct order of magnitude.

The analysis

Inertial bending torques

Let us examine the moment set up in a wing section a distance r from the wing base (Fig. 1) by a wing strip of mass dm, centred a distance r_i from the wing base, when the wing is subjected to an angular acceleration of $d^2\phi/dt^2$, where ϕ is the instantaneous angular position of the wing along the stroke plane (Ennos, 1989). The acceleration, a, of the strip is:

$$a = r_i d^2\phi/dt^2 \tag{1}$$

and this will require a force, f, where:

$$f = r_i dm\, d^2\phi/dt^2 . \tag{2}$$

This force acts at a distance $(r_i - r)$ from the wing section, so the moment set up there by the strip, dT_I, is

$$\begin{aligned} dT_I &= f(r_i - r) \\ &= r_i(r_i - r)dm\, d^2\phi/dt^2 . \end{aligned} \tag{3}$$

The total moment, T_I, set up is the sum of the torques produced by all the wing strips outboard of the wing section:

$$T_I = d^2\phi/dt^2 \sum_{r}^{R} r_i(r_i - r)dm . \tag{4}$$

The moment will decrease away from the base both because there will be fewer strips outboard of a given section, and because the moment arm $(r_i - r)$ of each strip that is outboard of the section will be shorter.

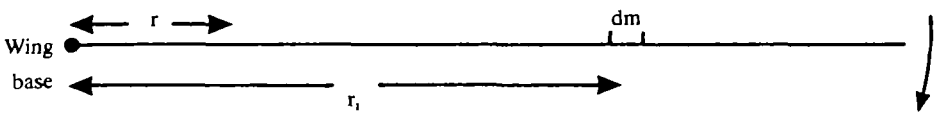

Fig. 1. A wing strip of mass dm a distance r_i from the wing base will produce a bending torque around the section which is a distance r from the base, when the wing is accelerated.

In Ennos (1989) the wings of each animal that had been filmed were subjected to strip analysis. The mass of each 2 mm wide strip parallel to the wing chord was found, as was the virtual mass of each 1 mm wide wing strip, equal to the mass of a 1 mm long cylinder of air with diameter equal to the local wing chord (Vogel, 1962). These strip masses were substituted into equation 4 to give the values of $\sum r_i(r_i - r)dm$ for wing sections at 1 mm intervals from the wing base, for both actual and virtual mass. The distance r_i was taken to be the distance from the wing base to the point halfway along each strip. The values at the base are equal to the moment of inertia, I_m, of wing mass $\sum r_i^2 dm$ and I_v of virtual mass $\sum r_i^2 dm_v$. The distribution of mass along the wing, as well as the total mass, will therefore govern the magnitude of the torques. The moment of inertia will be the same as if the mass were all concentrated a distance $\hat{r}_2(m)R$ from the wing base, where R is the wing length and $\hat{r}_2(m)$ is the second nondimensional radius of wing mass (Ellington, 1984*a*) and is given by the formula:

$$\hat{r}_2(m) = (\sum r_i^2 dm/mR^2)^{0.5} . \quad (5)$$

The nondimensional radii of mass, $\hat{r}_2(m)$, and virtual mass, $\hat{r}_2(v)$, were calculated from the strip masses (Ennos, 1989).

As it was assumed for the calculation that the wings followed simple harmonic motion, the maximum angular acceleration, $d^2\phi/dt^2_{max}$, at stroke reversal was estimated using the expression of Weis-Fogh (1973):

$$d^2\phi/dt^2_{max} = 2\pi^2 n^2 \Phi , \quad (6)$$

where n is the frequency and Φ the amplitude of the wingbeat in radians. The total maximum inertial torque, T_{Imax}, at the base is therefore given by:

$$T_{Imax} = 2\pi^2 n^2 \Phi (I_m + I_v) . \quad (7)$$

The moments of wing and virtual mass inertia, I_m and I_v, of each of the insects are given in Table 1, as are the total values of wing mass, m_w, and virtual mass, m_v, and the nondimensional radii of wing mass and virtual mass, $\hat{r}_2(m)$ and $\hat{r}_2(v)$.

The maximum inertial bending torque, T_{Imax}, is the sum of that due to mass and that due to virtual mass and was calculated using kinematic data from Ennos (1989) (Table 1).

It can be seen that the moment of inertia of the wing virtual mass is typically only slightly less than that of the wing mass, even though the wing virtual mass is generally less than half the wing mass. This is because the wing mass is concentrated nearer the base than the virtual mass, and $\hat{r}_2(m)$ is consequently lower than $\hat{r}_2(v)$. Fig. 2 is an example of the raw data from which the moments were calculated, showing the masses and virtual masses of wing strips for the hoverfly, *Eristalis tenax* Et.1. The concentration of wing mass at the base can clearly be seen.

The spanwise distribution of inertial bending torque was very similar in all the species studied, so the results for the hoverfly sequence Et.1a alone are shown (Fig. 3A). Bending torque falls extremely rapidly away from the wing base.

Table 1. *Inertial and aerodynamic moments about the wing base and torsional axis*

Insect	Sequence	m_w (μg)	m_v (μg)	$\hat{r}_2(m)$	$\hat{r}_2(v)$	I_m ($kg\,m^2 \times 10^{-12}$)	I_v ($kg\,m^2 \times 10^{-12}$)	T_{Imax} ($Nm \times 10^{-6}$)	T_{Amax} ($Nm \times 10^{-6}$)	T_{Pmax} ($Nm \times 10^{-6}$)
Eristalis tenax										
Et.1	a	370	117	0·42	0·512	8·57	4·14	11·9	5·89	0·38
	b							13·0	5·89	0·38
	c							12·3	5·89	0·38
Et.3	a	340	110	0·41	0·514	6·55	3·41	9·9	5·42	0·37
	b							10·7	5·42	0·37
Bibio marci										
Bm.1	a	224	134	0·45	0·531	5·66	4·75	5·1	3·96	0·27
	b							5·3	3·96	0·27
Bm.2		149	70	0·45	0·515	2·63	1·63	3·4	1·33	0·09
Calliphora vicina										
Cv.1		235	91	0·38	0·516	2·75	2·05	3·4	3·42	0·24
Cv.2								4·0	3·42	0·24
Cv.3								3·3	3·42	0·24
Cv.4								4·5	3·42	0·24
Conops strigata										
Cs.1		76	31	0·40	0·598	0·72	0·65	1·4	1·21	0·06
Tipula paludosa										
Tp.3		471	151	0·52	0·605	36·5	15·6	7·0	4·89	0·18

m_w, wing mass; m_v, virtual mass; $\hat{r}_2(m)$, second nondimensional radius of mass; $\hat{r}_2(v)$, second nondimensional virtual mass; I_m and I_v, moments of inertia about the base.

The maximum basal torques calculated for each sequence are given: inertial bending torque, T_{Imax}; aerodynamic bending torque, T_{Amax}; aerodynamic pitching torque, T_{Pmax}.

Aerodynamic bending torques

During each halfstroke the wing must also withstand the bending torques caused by the aerodynamic forces it produces: lift and drag. Using quasi-steady aerodynamics, and assuming that equal lift is produced during symmetrical hovering on the two halfstrokes, and that the wings are flapped with simple harmonic motion, these torques can be estimated.

The peak velocity in simple harmonic motion is $\sqrt{2}$ times the average velocity. Since lift is proportional to the square of velocity, the peak lift force, produced at midstroke, will be about twice the average lift. To hover, therefore, each wing will produce a peak lift force equal to the weight of the insect, mg. As aerofoils move through the air at relative angles of attack of less than 20°, this lift will act nearly at right angles to the wing chord, whereas the drag produced, generally a much smaller force, will act nearly parallel to the chord. Drag may therefore be conveniently ignored when calculating the peak force perpendicular to the wing chord, which will be approximately equal to the peak lift.

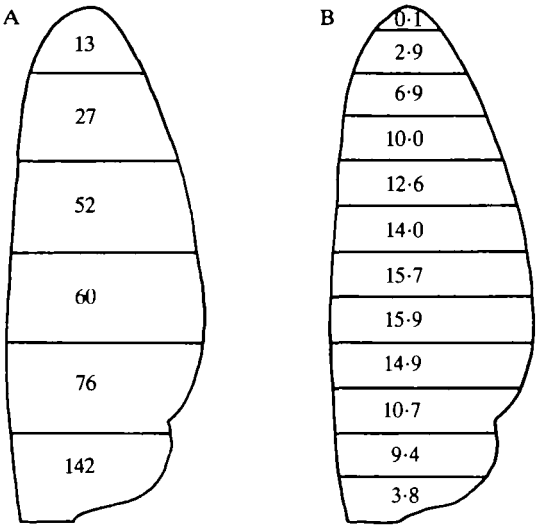

Fig. 2. The wing mass (A) and wing virtual mass (B) distribution of the hoverfly Et.1. The masses of wing strips are given in micrograms. Mass strips are 2 mm wide; virtual mass strips are 1 mm wide. Wing mass is concentrated near the wing base, virtual mass halfway along the wing.

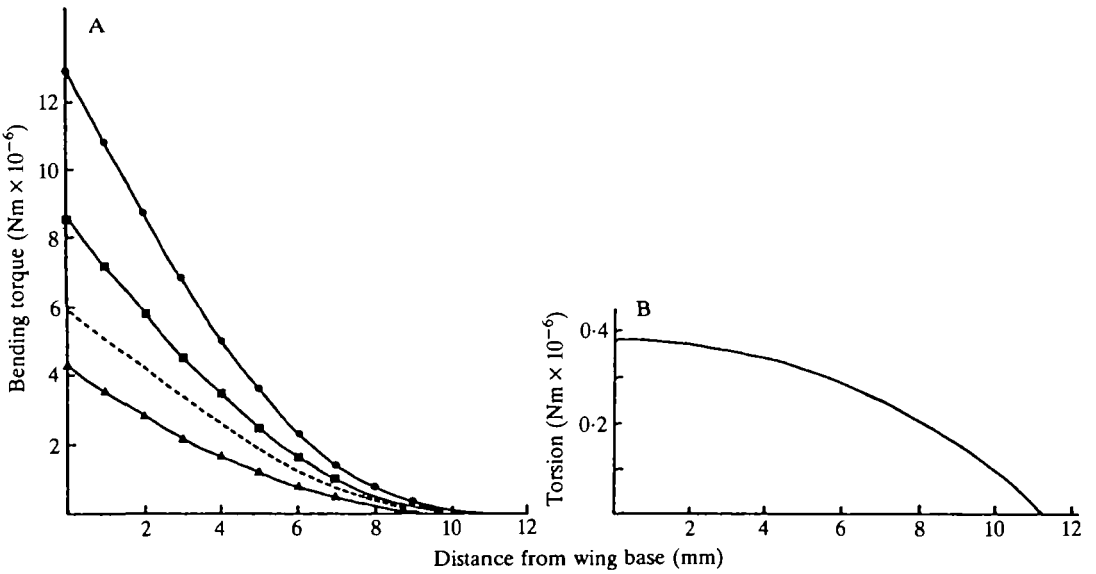

Fig. 3. The distribution of maximum torques along the wing of a hoverfly during the flight sequence Et.1a (Ennos, 1989). (A) Bending torques due to the inertia of the wing mass (■), the wing virtual mass (▲), to the total inertia of both wing mass and virtual mass (●), and to aerodynamic forces (---). The torque decreases rapidly away from the base. (B) Pitching torques about the spanwise torsional axis caused by aerodynamic forces. Although much smaller, the torque only decreases rapidly near the wing tip.

Since the local value of the lift is proportional to the square of the local velocity, the centre of pressure will be at the second radius of area, a distance $\hat{r}_2(s)R$ from the wing base, where R is the wing length and $\hat{r}_2(s)$ the second nondimensional moment of area (Ellington, 1984*a*). The maximum torque produced at the wing base, T_{Amax}, is therefore given by the expression:

$$T_{Amax} = mgR\hat{r}_2(s) . \quad (8)$$

Values of T_{Amax} were calculated from the data of Ennos (1989) (Table 1). It can be seen that aerodynamic bending torques are generally slightly less than those caused by inertia.

The spanwise torque distribution will be similar to that produced by inertial forces. More force will be produced by the faster-moving distal parts of the wing, just as they possess more inertia about the wing base. The moment will decrease rapidly away from the wing base for the same reasons: the smaller fraction of the wing outboard of the section, and the shorter moment arm of each force to the section.

The approximate torque distribution is shown in Fig. 3A for the sequence Et.1a of the hovering flight of the drone fly *Eristalis tenax* (Ennos, 1989).

Aerodynamic wing pitching torques

The aerodynamic forces produced by a wing section at the Reynolds numbers characteristic of insect flight are centred approximately one-quarter of the chord, c/4, back from the leading edge (Norberg, 1972; Ellington, 1984*c*). The torsional axis of the wing, along which forces will not cause pitch changes in the wing (Norberg, 1972), however, is usually closer to the leading edge. In the flies that I examined (Ennos, 1988*b*), it was typically only one-eighth of the wing chord, c/8, behind the leading edge. Aerodynamic forces will therefore act behind the torsional axis and tend to produce a nose-down pitching moment on it.

The magnitude of this moment at the wing base may be estimated, with the same assumptions as were made to calculate bending moments. The peak aerodynamic force on each wing is estimated to be the weight of the insect. It is assumed that this force acts at about 90° to the wing section at the quarter-chord point behind the leading edge, and so a distance of one-eighth of the mean chord, $\bar{c}$, behind the torsional axis. The torque produced around the torsional axis, T_{Pmax}, is therefore:

$$T_{Pmax} = mg\bar{c}/8 . \quad (9)$$

The mean wing chord is equal to the area of the wing pair, S, divided by twice the wing length, 2R, so equation 9 can be expressed as:

$$T_{Pmax} = mgS/16R . \quad (10)$$

The pitching moments at the base, given in Table 1, are typically less than one-twentieth of the magnitude of the bending moments.

The spanwise distribution of this torque will be quite different from that of the bending torques, since the moment arm, c/8, of each section remains high until

very near the tip, and does not decrease away from the base as does the moment arm for bending. Aerodynamic force production is greatest at the fast-moving wing tip during hovering, and falls to zero at the base, so most of the aerodynamic pitching torque about the torsional axis is set up near the wing tip. The torque will therefore decrease only gradually away from the base (Fig. 3B).

Discussion

Bending torques on insect wings decrease rapidly away from the base, values halfway along the wing being typically only about one-quarter of those at the base, and falling to zero at the tip. It is not surprising, therefore, that the wings of insects are thicker at the base than at the tip. Mass is concentrated near the base to resist the higher bending moments, and outer regions are as light as possible, to reduce the stress caused at the wing base and to reduce the energy expenditure involved in accelerating the wing, although much of the wing's energy is recovered in the flight muscles and thoracic box (Machin & Pringle, 1959; Ellington, 1984*d*). Torsional moments stay at a high value until near the wing tip, but are far smaller than bending moments.

The surprising aspect of the behaviour of the wings is that they twist but do not noticeably bend in flight, despite the fact that the bending torques on them are far larger than the pitching torques which tend to twist them by around 10° during each wingbeat. This is due to their open, corrugated structure (Ennos, 1988*a*), which combines high bending stiffness with low torsional stiffness.

The pitch of the wings also changes greatly between strokes. The very high torsional compliance of the wing base (Ennos, 1987) allows the inertia of the wing to cause rotation of over 90° at stroke reversal. The aerodynamic pitching torque can then maintain it at the correct pitch attitude during the next halfstroke.

I would like to thank Dr R. J. Wootton for his help and criticism during the production of the manuscript. The work was carried out while under tenure of an SERC research studentship.

References

DUDLEY, T. R. (1987). The mechanics of forward flight in insects. PhD thesis, University of Cambridge.

ELLINGTON, C. P. (1984*a*). The aerodynamics of hovering insect flight. II. Morphological parameters. *Phil. Trans. R. Soc. Ser.* B **305**, 17–40.

ELLINGTON, C. P. (1984*b*). The aerodynamics of hovering insect flight. III. Kinematics. *Phil. Trans. R. Soc. Ser.* B **305**, 41–78.

ELLINGTON, C. P. (1984*c*). The aerodynamics of hovering insect flight. IV. Aerodynamic mechanisms. *Phil. Trans. R. Soc. Ser.* B **305**, 79–113.

ELLINGTON, C. P. (1984*d*). The aerodynamics of hovering insect flight. VI. Lift and power requirements. *Phil. Trans. R. Soc. Ser.* B **305**, 145–181.

ENNOS, A. R. (1987). A comparative study of the flight mechanism of Diptera. *J. exp. Biol.* **121**, 355–372.

ENNOS, A. R. (1988*a*). The importance of torsion in the design of insect wings. *J. exp. Biol.* **140**, 137–160.

ENNOS, A. R. (1988*b*). The inertial cause of wing rotation in Diptera. *J. exp. Biol.* **140**, 161–169.
ENNOS, A. R. (1989). The kinematics and aerodynamics of the free flight of some Diptera. *J. exp. Biol.* **142**, 49–85.
MACHIN, K. E. & PRINGLE, J. W. S. (1959). The physiology of insect fibrillar muscle. II. Mechanical properties of a beetle flight muscle. *Proc. R. Soc. Ser.* B **151**, 204–226.
NORBERG, R. Å. (1972). The pterostigma of insect wings: an inertial regulator of wing pitch. *J. comp. Physiol.* **81**, 9–22.
PENNYCUICK, C. J. (1967). The strength of the pigeon's wing bones in relation to their function. *J. exp. Biol.* **46**, 219–233.
VOGEL, S. (1962). A possible role of the boundary layer in insect flight. *Nature, Lond.* **193**, 1201–1202.
WEIS-FOGH, T. (1973). Quick estimates of flight fitness in hovering animals, including novel mechanisms for lift production. *J. exp. Biol.* **59**, 169–230.
WOOTTON, R. J. (1981). Support and deformability in insect wings. *J. Zool., Lond.* **193**, 447–468.